PHYSICAL REVIEW VOLUME 130, NUMBER 6 15 JUNE 1963

Singularity of the Regge Amplitude*

J. N. ISLAM, P. V. LANDSHOFF,† AND J. C. TAYLOR
Department of Applied Mathematics and Theoretical Physics, University of Cambridge, Cambridge, England
(Received 7 February 1963)

It is shown that the Regge amplitude $a(l,s)$ has singularities at certain fixed, real, physical values of s for all nonphysical values of l. These singularities are not normal thresholds and are not singularities of the complete amplitude $A(s,t,u)$. They arise indirectly through unitarity. Their presence is deduced from the existence of a perturbation graph which satisfies the Mandelstam representation with spectral boundary curves having asymptotes other than the normal threshold lines.

1. INTRODUCTION

THE singularities of the Feynman integral corresponding to a given perturbation graph are given by Landau's equations.[1] It is widely believed that as a consequence of unitarity these singularities, or at least those of them that are on the physical sheet, also appear in the complete scattering amplitude, independently of perturbation theory.[2]

The solutions of Landau's equations have only been analyzed in detail for the simpler diagrams.[3] These include the square,[4] the square with one diagonal,[5] and the tetrahedron[6–8] of Fig. 1. Each of these satisfies the Mandelstam representation when the masses lie in a suitable range of values, but the third is more complicated than the other two in that it contributes to all three spectral regions and has normal thresholds in all three channels. Further, it has previously been noted[6] that the spectral boundaries for this diagram have other asymptotes in addition to the expected normal threshold lines. This result, when it was recently rediscovered in the course of some further work on the diagram,[8] at first sight was puzzling, as the Mandelstam representation appears to require that the asymptotes be singular lines for the graph, while they cannot be[9] because they may (for suitable values of the masses) traverse a physical region.

We give the resolution of this puzzle in Sec. 3. It has the corollary that for all nonphysical values of the angular momentum the Froissart-Gribov definition of the Regge amplitude[10] $a(l,s)$ has a singularity at the value s_A of s corresponding to one of the new asymptotes. This is explained in Sec. 4, where we also give the discontinuity of $a(l,s)$ associated with the branch point s_A.

As we have said, s_A represents a real, physical energy. We give two examples, the πN scattering graphs of Fig 2. For each of these in the πN channel $\sqrt{s_A}\approx m_p+3.6m_\pi$. By symmetry Fig. 2(a) has a similar asymptote in the other πN channel (u channel), but for Fig. 2(b) u_A lies above the $N\bar{N}N\pi$ threshold and we do not quote its actual value. In the $N\bar{N}\leftrightarrow 2\pi$ channel, Fig. 2(b) has $t_A=8m_p^2+8m_\pi^2$ but Fig. 2(a) has no asymptote apart from the four-pion normal threshold.

2. THE NEW ASYMPTOTES

In considering the Landau curve for the graph of Fig. 1 we shall use the symbols in the figure to label the masses (internal m, external M), momenta q, and Feynman parameters α on the lines.

In a special case (Appendix A) it is possible to obtain explicitly the positions of the asymptotes. In

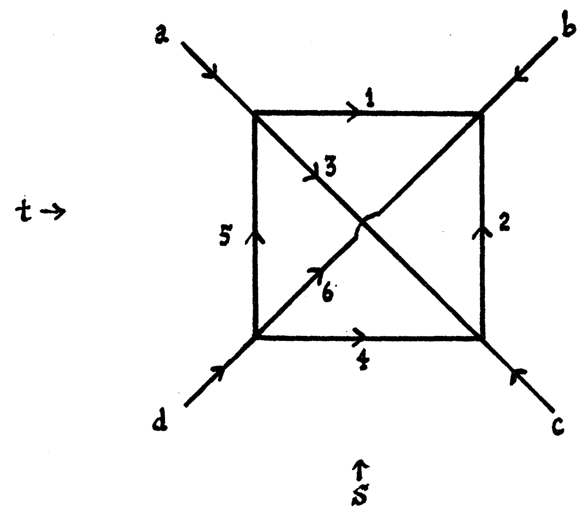

FIG. 1. The diagram with which the new asymptotes and singularities are connected.

---

* The research reported in this document has been sponsored in part by the Air Force Office of Scientific Research, OAR, through the European Office, Aerospace Research, United States Air Force.
† NATO Fellow.
[1] L. D. Landau, Nucl. Phys. **13**, 181 (1959).
[2] J. C. Polkinghorne, Nuovo Cimento **23**, 360 (1962); **25**, 901 (1962); H. P. Stapp, Phys. Rev. **125**, 2139 (1962).
[3] For general methods of analysis of Landau diagrams see R. J. Eden and J. C. Polkinghorne, in Lecture Notes 1, Brandeis University Summer School, 1961 (W. A. Benjamin, Inc., New York, 1962).
[4] J. Tarski, J. Math. Phys. **1**, 149 (1960).
[5] R. J. Eden, P. V. Landshoff, J. C. Polkinghorne, and J. C. Taylor, J. Math. Phys. **2**, 656 (1961).
[6] V. Kolkunov, L. Okun, and A. Rudik, Zh. Eksperim. i Teor. Fiz. **38**, 877 (1960) [translation: Soviet Phys.—JETP **11**, 634 (1960)]; V. Kolkunov, *ibid.* **40**, 678 (1961) [translation: *ibid.* **13**, 474 (1961)].
[7] D. I. Olive and J. C. Taylor, Nuovo Cimento **24**, 814 (1962).
[8] J. N. Islam (to be published).
[9] This follows from unitarity: see R. J. Eden, Phys. Rev. **119**, 1763 (1960); and also P. V. Landshoff, Phys. Letters **3**, 116 (1962).
[10] For a review of complex angular momenta see E. J. Squires, Lecture Notes, Cambridge, 1962 (unpublished). Further references are given here.

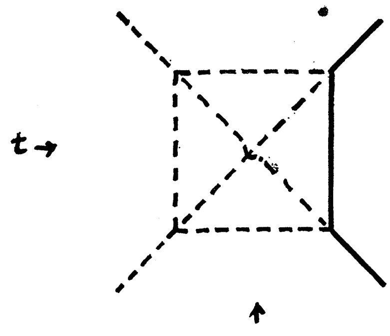

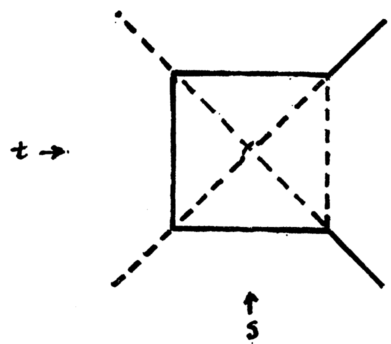

FIG. 2. Two particular cases of Fig. 1 for πN scattering.

the general case (Appendix B) we find implicit equations which can be solved for particular numerical examples. Some simple rules about the asymptotic behavior can also be deduced.

A detailed discussion is given in Appendix A for the special case in which

$$m_1=m_4,\quad m_2=m_5,\quad m_3=m_6,\quad \text{and}\quad M_a=M_b=M_c=M_d.$$

There is then a specially symmetric solution of the Landau equations for which

$$\alpha_1=\alpha_4,\quad \alpha_2=\alpha_5,\quad \text{and}\quad \alpha_3=\alpha_6.$$

This solution seems always to contain the whole of the spectral boundary. It is simple enough to be plotted numerically, and the asymptotes can be found analytically. The form of the relevant part of the Landau curve is drawn[11] in Fig. 3, as usual in the real (stu) plane. Normal thresholds are drawn as continuous lines and the other asymptotes as broken lines. In addition to the spectral boundaries (continuous curves), some other branches of the Landau curve, having the same asymptotes,[12] are drawn as dashed curves. The figure is drawn for the masses labeled so that $m_1>m_2>m_3$. Special cases where there are further equalities may be obtained in an obvious way. The normal threshold in the s channel is at

$$s_N=(2m_2+2m_3)^2,$$

while the new asymptote is at

$$s_A=8(m_2^2+m_3^2)\geq s_N.$$

General mass values are considered in Appendix B. Guided by the previous special case, one seeks a point on the Landau curve for which s is finite, t is infinite, and $\alpha_1=\alpha_4=0$. One such point corresponds to the expected normal threshold asymptote, but there is another in which the momenta q_1 and q_4 are infinite but the products $\alpha_1 q_1$ and $\alpha_4 q_4$ remain finite and nonzero. This makes $t\to\pm\infty$ according as $m_3m_6\gtrless m_2m_5$, so that the general form of the curves is again as in Fig. 3 provided that

$$m_1m_4>m_2m_5>m_3m_6. \tag{1}$$

Otherwise, their form is obtained by appropriate interchanges of the variables s, t, and u.

The positions of the new asymptotes are not easy to determine explicitly in the general case. But they have the interesting property that, for instance, s_A is a function of m_2, m_5, m_3, and m_6 only. In other words, the position of the asymptote depends only on the particles into which the system may dissociate in the corresponding channel. In this respect it is similar to a normal threshold.

Two other properties are worth noting. First, $s_A\geq s_N$ with equality if and only if $m_2m_5=m_3m_6$. Second, because[3]

$$\frac{ds}{dt}=\frac{\alpha_1\alpha_4(\alpha_3\alpha_6-\alpha_2\alpha_5)}{\alpha_2\alpha_5(\alpha_1\alpha_4-\alpha_3\alpha_6)},$$

it follows that ds/dt changes sign at the asymptote, since α_1, α_4, and (it is shown in Appendix B) $(\alpha_3\alpha_6-\alpha_2\alpha_5)$ all vanish there. Thus, the behavior near the asymptote is like $y=1/x^2$ rather than like $y=1/x$.

3. THE CONSISTENCY OF THE MANDELSTAM REPRESENTATION

The broken curves in Fig. 3 cannot be parts of the boundary of the spectral region, since they lead outside the regions of the crossed normal threshold cuts[3] and there need not be any anomalous thresholds. The dispersion relation for the absorptive part in the s channel is, therefore,

$$A_s(s,t)=\frac{1}{\pi}\int_{-\infty}^{f(s)}\frac{dt'\,\rho_{st}(s,t')}{t'-t},\quad s_N<s<s_A, \tag{2}$$

$$=\frac{1}{\pi}\int_{-\infty}^{f(s)}\frac{dt'\,\rho_{st}(s,t')}{t'-t}+\frac{1}{\pi}\int_{g(s)}^{\infty}\frac{dt'\,\rho_{su}(s,t')}{t'-t},\quad s_A<s. \tag{3}$$

[11] We take the masses to be such that anomalous thresholds and acnodes do not occur. See reference 8.

[12] These branches actually only have the form shown if $M^2<m_1^2+m_2^2+m_3^2+2m_2m_3+2m_3m_1-2m_1m_2$.

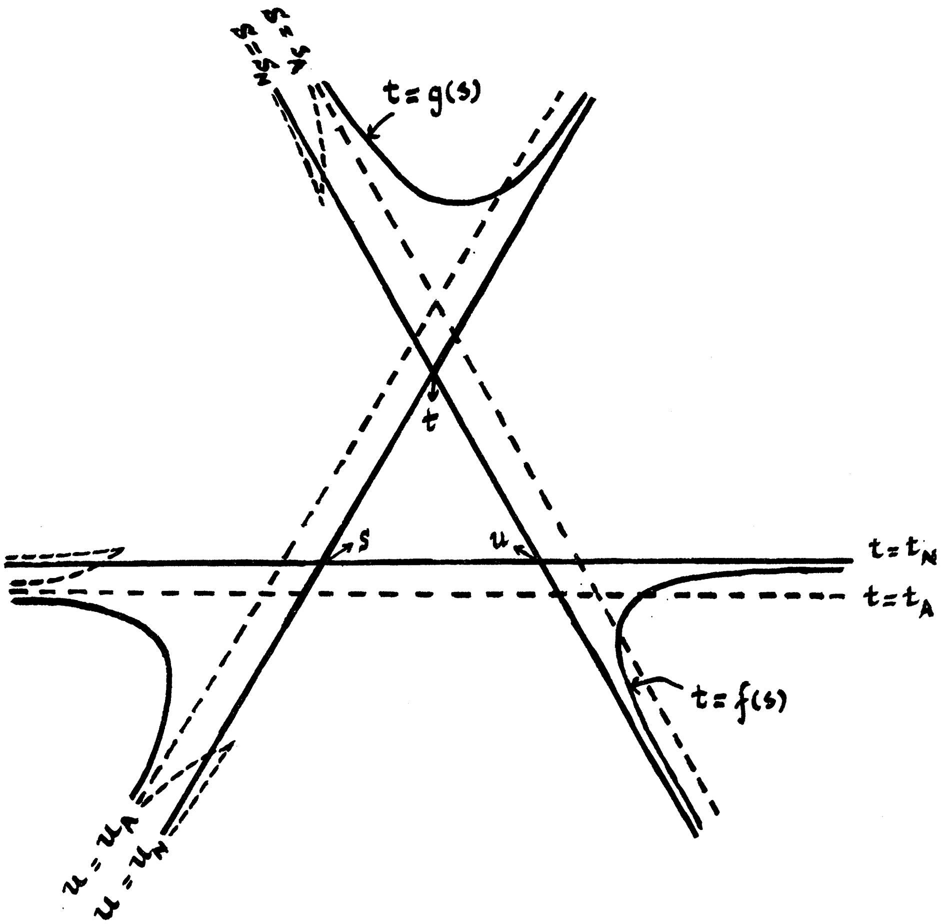

FIG. 3. The spectral function boundary curves for Fig. 1, when $m_1m_4>m_2m_5>m_3m_6$. Other portions of the Landau curve are shown as broken curves. Continuous lines represent normal thresholds and broken lines represent the new asymptotes.

Here we have assumed the Mandelstam representation without subtractions; subtractions would be an inessential complication. In (2) and (3)

$$t=f(s) \quad \text{and} \quad t=g(s)$$

are, respectively, the equations of the boundaries of the *st* and *su* spectral regions.

Because form (3) differs from (2), it seems as if $A_s(s,t)$ has a singularity at $s=s_A$. However, this cannot be,[9] because the line $s=s_A$ is independent of the external masses and so can traverse the physical region for the s channel when the latter are sufficiently small.

The resolution of the difficulty[13] is that $t=g(s)$ is actually a singularity of ρ_{st}. It is on an unphysical sheet for $s<s_A$ and, as the expression (2) is continued through $s=s_A$, it passes through the point $t=\infty$ and on to the physical sheet. But $t=\infty$ is an end point of the integration in (2), and so the singularity forces one to distort the contour of integration. This results in an extra integral, which is the second integral in (3).

The behavior here is, in fact, quite similar to that in a situation which is already familiar. This is the process by which an anomalous threshold appears in the amplitude $A(s,t)$ as one of the external masses M is increased through the critical value M_c. For $M<M_c$ the dispersion relation for $A(s,t)$ involves an integral over the normal threshold cuts, but as M is increased through M_c one must add an extra integral from the anomalous threshold to the normal threshold. However, M_c is not a singularity of the amplitude regarded as a function of s, t, and M, and in a similar way s_A is not a singularity of $A_s(s,t)$ in the problem under discussion. But $s=s_A$ *is* a singularity of the Regge amplitude. This is explained in the next section and a more detailed analysis of the distortion of contours of integration is given.

[13] We are very indebted to Professor S. Mandelstam and Dr. J. C. Polkinghorne, who helped to provide the key to the understanding of this problem.

4. THE REGGE AMPLITUDE

We recall the Froissart-Gribov definition[10] of the Regge amplitude. For physical values of l the partial-wave amplitude is

$$a(l,s)=\frac{1}{2}\int_{-1}^{1} A(s,t)P_l(z)dz \tag{4}$$

FIG. 4. The broken line represents a path in the s plane round the branch point at s_A, when the normal threshold cut is pulled aside.

$$=\frac{1}{\pi}\int_{t=t_N}^{t=\infty} A_t(s,t)Q_l(z)dz$$
$$-\frac{1}{\pi}\int_{u=u_N}^{u=\infty} A_u(s,t)Q_l(z)dz. \quad (5)$$

As before, t_N and u_N are the normal thresholds in the t and u channels, respectively. The form (5) is not suitable for continuation to unphysical values of l because the second term does not have the correct asymptotic behavior for the Watson-Sommerfeld transformation. This is because it is an integral of $Q_l(z)$ over negative values of z. Therefore, one replaces $Q_l(z)$ in the second term by $\mp Q_l(-z)$, so that the Froissart-Gribov amplitudes

$$a_{\mathrm{FG}}^{\pm}(l,s)=\frac{1}{\pi}\int_{t=t_N}^{t=\infty} A_t(s,t)Q_l(z)dz$$
$$\pm\int_{u=u_N}^{u=\infty} A_u(s,t)Q_l(-z)dz \quad (6)$$

do have the right asymptotic behavior and are equal to the form (4), respectively, for even and odd integral values of l [provided the integrals in (6) converge]. A theorem of Carlson[10] guarantees that they are the only functions with these properties.

We now show that the functions in (6) have a singularity at $s=s_A$ for the values of l for which they are not equal to (4). The functions $a_{\mathrm{FG}}^{\pm}$ each have the normal threshold singularity $s=s_N$. If, as usual the corresponding cuts are drawn along the positive real axis in the s plane, then for any value of s not on the real axis in the cut s plane the functions A_t, A_u, respectively, have no singularities for real t and real u. This follows from the Mandelstam representation. Hence, if the contours of integration of the two integrals in (6) are taken, respectively, as the real t, u axes, no singularity of either integrand will cross the contours as s is varied in the cut s plane. Hence, the form (6), with real, undistorted t, u contours, is analytic provided s is kept away from the real cut.[14]

We now examine what happens if we do cross the cut or, more conveniently, push it back so that it no longer runs along the real axis. We shall show below that if we start with the form (6) with undistorted contours at the point P in Fig. 4 and continue along the path shown to the point Q, we must distort the contours. Thus, at Q we have

$$a^{\pm}(l,s)=a_{\mathrm{FG}}^{\pm}(l,s)+f^{\pm}(l,s), \quad (7)$$

[14] We are grateful to J. R. Taylor for insisting on this argument.

where $a_{\mathrm{FG}}^{\pm}$ again represents the form (6) with undistorted contours. We conclude that $s=s_A$ is a branch point of the Regge amplitude and has a cut attached to it (as drawn in Fig. 3, for example). The discontinuity across this cut is $f^{\pm}(l,s)$.

Let us rewrite the integrals in (6):

$$\frac{1}{\pi}\int_{C_1} A(s,t)Q_l(z)dz\pm\int_{C_2} A(s,t)Q_l(-z)dz, \quad (8)$$

where, as before, $A(s,t)$ is the complete amplitude. It is convenient to draw the undistorted contours C_1, C_2 in the τ plane, where

$$\tau=1/t,$$

so that $t=\infty$ becomes the finite point $\tau=0$. This is done in Fig. 5. The position of the point $u=u_N$ in the t plane varies with the value chosen for s, but this will not affect us here.

In Fig. 6, again in the τ plane, we plot the path of the point $t=g(s)$ as s is varied from P to Q. As indicated at the end of Sec. 2, $t=g(s)$ in the neighborhood of $s=s_A$ behaves like

$$t=-k/(s-s_A)^2.$$

This is shown explicitly for the symmetrical mass case in Appendix A [see Eq. (A6)]. If we represent the path PQ by $s=s_A+\sigma-i\epsilon$, where σ varies, this becomes

$$\tau=-k(\sigma^2-\epsilon^2-2i\sigma\epsilon),$$

so that the path is as sketched in Fig. 6.

We assert that when we reach $s=Q$ the singularity we plot in Fig. 6 has emerged through the right-hand cut in the t or τ plane. This is because for $s>s_A$ the curve $t=g(s)$ is the Mandelstam spectral curve and it is, therefore, a singularity of the amplitude $A(s,t)$ in the limit in which we have approached it. Thus, at Q the contour C_1 is distorted, as drawn in Fig. 7(a). Although we do not have to, we may also distort C_2, as in Fig. 7(b). Then we have arrived at the form (7), with

$$f^{\pm}(l,s)=\frac{1}{\pi}\int_C [Q_l(z)\pm Q_l(-z)]A(s,t)dz, \quad (9)$$

where C is the contour drawn in Fig. 7(c). Evidently f^+ vanishes for even integral l and f^- for odd integral l (provided the integrals converge), but not otherwise. Hence, the continuation of $a^{\pm}(l,s)$ is still equal to the form (4) for these values of l. This mean that Carlson's theorem requires $f(l,s)$ to have the "wrong" asymptotic

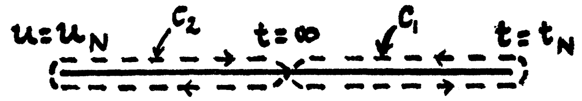

FIG. 5. Cuts in the τ plane ($\tau=t^{-1}$) and the integration contours (broken lines) in Eq. (9), when s is at P in Fig. 4.

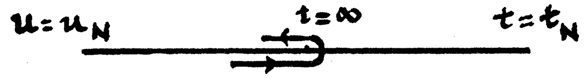

FIG. 6. The path of $t=g(s)$ in the τ plane when s moves from P to Q in Fig. 4. The singularity comes onto the physical sheet through the right-hand cut.

behavor, which may immediately be verified by inspection of (9).

5. CONCLUSION

We have shown that $s=s_A$ is a singularity of the Regge amplitude. It is, therefore, perhaps also a singularity of the Regge trajectory $l=\alpha(s)$, since this represents a pole of $a(l,s)$. It would seem difficult, however, to verify the existence of the singularity experimentally,[15] just as the inelastic normal thresholds have so far not produced any striking effects experimentally. It is not clear what effect its presence would have on the unitarity condition, were one able to write down inelastic unitarity for the Regge amplitude. s_A is not a singularity of the complete amplitude $A(s,t)$. The mechanism by which it is absent is somewhat delicate and this may be relevant in future practical calculations. If an approximation is made for the ρ_{st} spectral function care must be taken in the neighborhood of $s=s_A$, $t=\infty$; otherwise the line $s=s_A$ might emerge as a spurious singularity of the amplitude.

There may be other graphs with similar properties. Certainly there is the graph of Fig. 1 with some or all of the internal particles replaced by sets of particles.

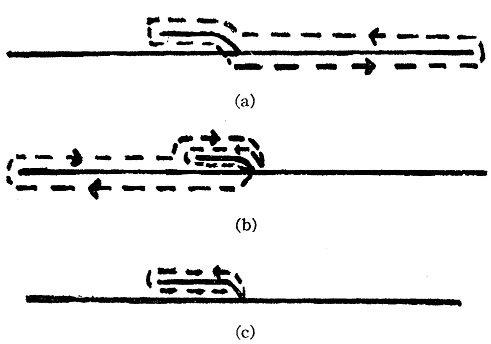

FIG. 7. Cuts and contours for s at Q in Fig. 4. (a) The distorted contour corresponding to C_2 in Eq. (9). (b) A possible way of drawing C_1 in Eq. (9). (c) The contour C in Eq. (10), representing the difference between Fig. 5 and the sum of Figs. 7(a) and (b).

ACKNOWLEDGMENTS

We are grateful to many of our colleagues for discussions. In addition to those in references 13, 14, and 15 we should like to mention particularly, I. Drummond and Dr. R. J. Eden. One of us (J. N. I.) is grateful to Cambridge University for a Research Maintenance Grant.

[15] We are grateful to Professor G. F. Chew for a discussion of this point.

APPENDIX A

In this Appendix we discuss the special case described in the third paragraph of Sec. 2. The symmetrical solution with $\alpha_1=\alpha_4$, $\alpha_2=\alpha_5$, and $\alpha_3=\alpha_6$ is not the only solution of Landau's equations, but it always seems to contain all the spectral boundary curves. For the very special case, $m_1=m_4=m_2=m_5$, $m_3=m_6=M=M_a=M_b=M_c=M_d$, this result can be proved by an application of a method of Patashinshi,[16] since it can be shown that only the symmetrical solution has all α positive.

The Landau curve is conveniently described in terms of the parameters x_1, x_2, x_3, where, for instance, $x_1m_2m_3$ is the scalar product of the momentum on either of the lines m_2 with that on either of the lines m_3. Landau's equations reduce to just two conditions:

$$m_2m_3x_1+m_3m_1x_2+m_1m_2x_3=\tfrac{1}{2}(M^2-m_1^2-m_2^2-m_\circ^2), \quad \text{(A1)}$$

corresponding to momentum conservation at any vertex; and

$$x_1^2+x_2^2+x_3^2+2x_1x_2x_3=1, \quad \text{(A2)}$$

the co-planarity condition for any of the triangular closed-loops in the diagram. The Mandelstam variables are given by

$$s=2(m_2^2+m_3^2)+8m_2m_3x_1+2m_3^2(x_1^2-x_2^2)/(1-x_3^2)+2m_2^2(x_1^2-x_3^2)/(1-x_2^2), \quad \text{(A3)}$$

with similar equations for t and u.

The foregoing equations are immediate generalizations of the work of references 6 and 8.

From (A3) we see that for an asymptote either one of the x's is equal to ± 1 or one or more is infinite. It turns out that the first alternative corresponds to a normal threshold. For the second alternative, Eqs. (A1) and (A2) only allow

$$x_2,\, x_3\to\infty, \quad x_2/x_3\to -m_2/m_3,$$
$$x_1\to(m_2^2+m_3^2)/2m_2m_3\geq 1, \quad \text{(A4)}$$

and the two other cases obtained by cyclic permutation of suffices. From (A3) and (A4) it follows immediately that

$$s\to s_A=8(m_2^2+m_3^2),$$

thus giving the position of the asymptote quoted in Sec. 2.

It also follows from Eq. (A4) and the expression for t that

$$t\sim 2m_1^2(x_2^2-x_3^2)/(1-x_1^2),$$

and, therefore, that $t\to\pm\infty$ according as $m_3\gtrless m_2$. Figure 3 has been drawn in accordance with this rule.

APPENDIX B

In this Appendix we construct the equations governing the asymptotes for general values of the masses.

[16] A. Z. Patashinshi, Zh. Eksperim. i Teor. Fiz. **39**, 1744 (1960) [translation: Soviet Phys.—JETP **12**, 1217 (1961)].

We also determine where the spectral curves approach new asymptotes and where they approach normal thresholds.

We use the same notation as in Sec. 2, and also write $q_{ij}=q_iq_j$ and $\beta_i=m_i\alpha_i$. The Landau equation for the loop 123 leads to

$$q_{13}=(\beta_1^2+\beta_3^2-\beta_2^2)/2\alpha_1\alpha_3, \tag{B1}$$

and there are corresponding expressions for q_{12}, q_{16}, q_{26}, q_{34}, q_{45}, q_{46}, q_{56}, and, except for an over-all change of sign, for q_{23}, q_{24}, q_{35}, q_{15}. Momentum conservation at the vertex $a135$ gives

$$M_a^2=m_1^2+m_3^2+m_5^2+2q_{13}-2q_{15}-2q_{35}, \tag{B2}$$

and there are similar equations for the other three vertices.

As explained in Sec. 2, we seek a point for which $\alpha_1=\alpha_4=0$ and $t=\infty$, because these conditions were fulfilled by the special case in Appendix A. Equations (B1) and (B2) then impose the following conditions on the remaining α's:

$$\begin{aligned}(\beta_2^2-\beta_6^2)/\alpha_2+(\beta_3^2-\beta_5^2)/\alpha_3&=0,\\(\beta_5^2-\beta_3^2)/\alpha_5+(\beta_6^2-\beta_2^2)/\alpha_6&=0,\\(\beta_2^2-\beta_3^2)/\alpha_2+(\beta_6^2-\beta_5^2)/\alpha_6&=0,\\(\beta_5^2-\beta_6^2)/\alpha_5+(\beta_3^2-\beta_2^2)/\alpha_3&=0.\end{aligned} \tag{B3}$$

We reject the obvious solution $\beta_2^2=\beta_3^2=\beta_5^2=\beta_6^2$ which is readily shown to yield the normal thresholds. Equation (B3) are seen to possess another solution in which

$$\alpha_2\alpha_5=\alpha_3\alpha_6, \tag{B4}$$

an equation used in Sec. 2. Since we are concerned with a portion of the Landau curve on which the α's are positive,[3] (B3) implies either that

$$\beta_2\geq\beta_6,\quad \beta_2\geq\beta_3,\quad \beta_5\geq\beta_6,\quad \beta_5\geq\beta_3, \tag{B5}$$

or the reverse inequalities throughout. Using (B4) one sees that (B5) or the reverse obtains according as $m_2m_5\gtrless m_3m_6$; and that if $m_2m_5=m_3m_6$ all four β's must be equal, so that the new asymptote coincides with the normal threshold.

The Landau condition for the loop 2356 implies

$$\alpha_2q_{25}=\alpha_6q_{56}-\alpha_3q_{35}-\alpha_5m_5^2. \tag{B6}$$

If we use expressions for q_{56} and q_{35} analogous to (B1) and the conditon $\alpha_1=\alpha_4=0$, (B6) becomes

$$q_{36}=(\beta_3^2+\beta_6^2)/2\alpha_3\alpha_5. \tag{B7}$$

With the help of (B7) and a similar expression (apart from a sign) for q_{25}, one can compute s:

$$\begin{aligned}s_A&=m_2^2+m_3^2+m_5^2+m_6^2\\&\quad+2(q_{25}-q_{23}+q_{26}-q_{35}-q_{36}+q_{56})\\&=(m_2+m_3+m_5+m_6)^2+\sum_{\substack{i>j\\ i,j=2,3,5,6,}}\frac{(\beta_i-\beta_j)^2}{\alpha_i\alpha_j}.\end{aligned} \tag{B8}$$

Equation (B3) and (B8) are the implicit equations for the asymptotes. Equation (B8) implies that $s_A\geq s_N$ with equality only if $m_2m_5=m_3m_6$ when the β's are all equal.

The asymptotic form for t may be got similarly. The dominant contribution comes from q_{14}, which may be computed from the Landau condition for the loop 1245, and one obtains

$$t\sim 2q_{14}=(\beta_3^2+\beta_6^2-\beta_2^2-\beta_5^2)/\alpha_1\alpha_4. \tag{B9}$$

On the spectral curve side of the asymptote α_1 and α_4 are positive and, therefore, from (B5) and (B9) $t\rightarrow\pm\infty$ according as $m_3m_6\gtrless m_2m_5$.

The special cases given at the end of the Introduction are obtained as follows. For Fig. 2(a), $m_3=m_5=m_6$ and Eqs. (B3) can be satisfied with $\beta_3=\beta_6$, reducing them to a cubic equation for the ratio β_5/β_3 together with Eq. (B4). This easily gives the numerical results stated. For Fig. 2(b) one requires the analog of (B3) for the t channel. One then has $m_1=m_4$, $m_3=m_6$ and can satisfy the equations simply with $\alpha_1=\alpha_4=\alpha_3=\alpha_6$. Insertion in the analog of (B8) gives

$$t_A=8(m_1^2+m_3^2),$$

just as in Appendix A. This, of course, is a consequence of the fact that the position of the asymptote depends only upon the four particles in the intermediate states of a given channel, not upon the remaining masses.